symmetry

MDPI

Article

Dimensional and Numerical Approach to Heat Transfer in Structural Elements with a Symmetrical Cross Section

Betti Bolló [1], Ioan Száva [2], Ildikó-Renáta Száva [3], Teofil-Florin Gălățanu [3,*], Károly Jármai [1] and Denisa-Elena Muntean [2]

[1] Institute of Energy Engineering and Chemical Machinery, University of Miskolc, H-3515 Miskolc, Hungary; betti.bollo@uni-miskolc.hu (B.B.); karoly.jarmai@uni-miskolc.hu (K.J.)
[2] Faculty of Mechanical Engineering, Transilvania University of Brasov, 29, Eroilor Avenue, 500 034 Brasov, Romania; eet@unitbv.ro (I.S.); denisa.popica@unitbv.ro (D.-E.M.)
[3] Faculty of Civil Engineering, Transilvania University of Brasov, 29, Eroilor Avenue, 500 034 Brasov, Romania; ildiko.szava@unitbv.ro
* Correspondence: galatanu.teofil@unitbv.ro

Abstract

The structures of buildings employ elements with symmetrical cross sections (columns have two axes of symmetry, and connecting beams have at least one), leading to symmetrical states of stress and deformation under the action of mechanical and thermal loads. Thermal stresses, resulting from temperature variations and fires, must be taken into account during calculations. Thus, it is important to perform theoretical and experimental studies on the propagation of heat flux during fires. Experimental investigations on prototypes can be replaced by investigations into attached, reduced-scale models. With the help of the model law (ML), deduced by dimensional approaches, the results obtained by the model can be extrapolated to the prototype. In the present article, the Szirtes' Modern Dimensional Analysis (MDA) method is proposed; this is a simple, reliable, and repeatable dimensional approach. By applying the MDA to both the structural elements and model of an entire industrial hall, in terms of thermal field propagation, the authors demonstrate the undeniable effectiveness of the method in these construction calculations. MDA enables the efficient and easy analysis of thermal states of the homologous points of the prototype, even for spatial structures.

Keywords: symmetric cross-sectional structural element; heat flow; modern dimensional analysis; thermal load-bearing capacity; finite element analysis; building safety

Academic Editor: Alice Miller

Received: 26 April 2025
Revised: 19 June 2025
Accepted: 8 July 2025
Published: 8 August 2025

Citation: Bolló, B.; Száva, I.; Száva, I.-R.; Gălățanu, T.-F.; Jármai, K.; Muntean, D.-E. Dimensional and Numerical Approach to Heat Transfer in Structural Elements with a Symmetrical Cross Section. *Symmetry* **2025**, *17*, 1271. https://doi.org/10.3390/sym17081271

1. Introduction

In construction, structural resistance elements (especially metallic ones, which are the subject of this paper) have cross sections that are either double symmetrical or at least simple symmetrical. This means that all supporting columns are cross sections with two axes of symmetry and that the connecting elements (cross beams or connecting beams) have at least one axis of symmetry, with one corresponding to the vertical direction. This characteristic enables these resistance frames to accept the applied loads, whether mechanical or thermal, in an optimal manner. Additionally, thanks to these special cross sections, an optimal stress–strain state can be ensured; this is in addition to obtaining the maximum strength and stiffness while consuming the least amount of material.

According to the strength of materials, a bar with a cross section with at least one axis of symmetry under the action of a thermal field (or a thermal rate) will present

symmetrical stress and strain states, which represents an undeniable advantage in the field of construction.

On the contrary, if the cross section of the structural elements (especially the resistance ones) is asymmetric, the action of mechanical or thermal loads will lead to the appearance of asymmetric stress and strain fields, leading to a behavior that is difficult to predict (civil or industrial constructions).

This is why the authors focus their attention on studying these symmetrical cross sections when subjected to the action of a specific thermal flow. Throughout their work, they take into account these significant aspects of structural resistance elements.

Starting with a detailed study on the effect of the controlled heating of well-defined segments of these structural elements, which are considered to be columns (supporting columns) in some industrial halls, the authors formulate a series of useful conclusions on fire resistance, a particularly important aspect of construction/buildings.

Civil engineers currently face the following challenge: the fire resistance of buildings is closely related to the heat transfer properties of structural elements. Consequently, adequate fire protection can be provided if precise information on their heat transfer behavior is available.

As the temperature increases, the load-bearing capacities of structural elements decrease significantly.

Consequently, the first step in enhancing the load-bearing capacity of the given structural element or structure involves obtaining precise information on its heat transfer properties during both real and simulated fires.

An important clarification, as is known, is that modelling fire phenomena, regardless of the type of modelling, represents a particularly complex problem, as has been noted in a succinct analysis of the specialist literature in the field. The authors, in their first attempt to address this phenomenon, chose to focus on the problem of heat transfer along steel structural elements, due to the concentration of the heat source (almost considered to be a point source), and located their base. In this particular case, they deduced, applied, and validated two model laws; these were based on Modern Dimensional Analysis (MDA) and developed by Szirtes [1].

It should be mentioned that the classical approach, which takes into account the entire complex phenomenon of combustion and the conditions in which fires occur, was not the focus of the authors of this paper.

However, this will be addressed in the future by a wider group of researchers, as this is a particularly complex phenomenon.

In this paper, the authors only wanted to highlight the various tools provided by this new approach, i.e., MDA, which, at least for this type of heat transfer problem/phenomenon in symmetrical cross-sectional beams with two axes, provided a model that was rigorously verified and validated by the authors based on detailed experimental investigations.

Thereby, to evaluate the real structural elements or the real structure's behavior, particularly their heat transfer properties and their fire resistance, the researchers focus on two main directions: they either perform high-accuracy experimental investigations on these large elements/structures, or exploit the advantages of dimensional methods.

In the first case, these experimental investigations involve numerous highly qualified persons, expensive equipment, and the consumption of significant time and money. One must also mention the challenges faced regarding the repeatability of the experiments conducted and the large size of the test benches required, such as the need for testing rooms. Consequently, this approach has become relatively disadvantageous.

In the second case, with the involvement of dimensional methods, all experimental investigations can be performed exclusively on attached reduced-scale models. The results

obtained by the models, using the mathematically deduced MLs, are transferred to the real structural element (or real structure), which predicts these latter behaviors. Thus, several of the challenges associated with the first approach automatically disappear.

From the literature briefly analyzed below, the authors have selected some useful information related to the topics addressed by fire specialists, particularly those applying the advantages of current dimensional methods in their work.

In [2], the authors validated the fire resistance and the load-bearing capacity of a steel frame using three numerical simulation approaches, namely SAFIR, Autodesk Simulation Mechanical, and ABAQUS, with similar results. Via the experimental validation of these numerical approaches, they obtained useful conclusions concerning the predicted fire resistance and load-bearing capacity of structures.

The authors of [3] provide useful details regarding the optimal application, based on European standards, of intumescent paints to the structural elements of buildings, taking into account the required fire resistance, shape factor, and critical temperature of the steel members.

In [4], the authors propose an alternative model for the estimation of the gas temperature in an enclosure based on the energy balance, as well as an empirical relation for vent flow. This model exhibits good flexibility in choosing the main variables, such as the material of the wall and the dimensions of the given enclosure/vent. It offers a more practical approach than the simpler McCaffrey–Quintier–Harkleroad (MQH) correlation.

The ventilation flow formula takes into account a wider range of conditions than the simpler MQH correlation. Although the model gives values that differ from the MQH values, it can be applied over a wider temperature range and represents a more flexible approach.

It enables one to predict the maximum temperature rise for a given fire scenario. By applying this approach, it is possible to solve other problems, such as flashover. In addition, it is possible to analyze the time-dependent heat release rate.

In order to predict the temperature of fires in rooms with the existing correlation methods, the authors of [5], based on a database comprising over 500 data points obtained from fire tests in 250 rooms, performed a useful analysis. They also proposed some new approaches based on a simple energy balance.

They also demonstrated that the McCaffrey–Quintier–Harkleroad (MQH) method provides a better prediction than the approach proposed by the authors, with respect to fires that are naturally ventilated by a single opening.

The authors conclude that their approach is useful when the burning rate cannot be approximated well or when there is an opening for ventilation. For these cases, they suggest that some assumptions should be accepted and that, based on the proposed effective approach, the necessary calculi should be performed. The authors of [6] performed a deep theoretical and experimental analysis of the thin fire protection blankets used in houses during wildfires. By performing several tests on different combinations of material, they obtained some efficient solutions. They also found that the effect of convective heating is more difficult to prevent than that of radiant heating.

In [7], the authors performed experimental investigations on full-scale unprotected and thermally protected composite cellular beams (steel and concrete) with regard to alterations in their mechanical properties during and after based on international fire norms fire.

These alterations, monitored via standard mechanical tests, resulted in a maximum decrease of 65% in the ultimate strain value of unprotected samples, which was much higher than that in protected samples. Based on these results, the authors proposed useful thermal protection solutions.

The author of [8] performed an analysis of scale modelling during fires, based on his extensive experience in the field. The first issue he addressed was scale modelling in air, followed by a brief analysis of scale modelling with salt and fresh water in order to analyze the movement of smoke. By analyzing their dimensionless groups for fire, the author described the partial scaling problems of some special fire scenarios. Several fire scenarios described for steel members and structures, tested at various scales, represent useful examples for the analysis and modelling of interesting and practical cases.

The authors of [9] scaled a fire problem using a set of dimensionless parameters/variables, taking into consideration the geometry, boundary conditions, and thermophysical properties of the materials. The numerical results obtained for two different powers of fire were compared in terms of their temperature profile and velocity in order to validate the proposed numerical models and improve them, especially for real-scale cases.

The author of [10] provides a very useful introduction to the scaling of thermal phenomena, based on multiple theoretical and experimental investigations.

In addition, in [11], the same author provides a detailed and useful analysis of scaling in fire phenomena, based on three main techniques; these are Froude, analogue, and pressure modelling. The dimensionless groups deduced for a wide range of fire phenomena, which are described, illustrated, and based on a meticulous review of the literature, represent a useful tool for specialists. The phenomena analyzed and methodologies described can represent a solid starting point for any fire specialist planning future research in the field. The authors of [12] offer a useful synthesis of the actual approaches employed in the scale modelling of several natural disasters and structural failure, with respect to the problems caused by fire. This valuable contribution can be applied to both engineering design and performance evaluation, and can enhance knowledge regarding fire phenomena and suitable modelling. The scaling laws that are presented and analyzed here will serve as a solid basis for the further numerical simulation of fire phenomena. It must also be mentioned that the presented scaling laws, validated by rigorous experimental investigations, represent the cornerstone of effective modelling.

Based on the analysis performed by the authors of this contribution, it is clear that not all dimensional methods offer an optimal research approach; this is particularly in the case of symmetrical cross-sectional structural elements, which are briefly analyzed below.

2. Briefly About the Dimensional Methods

Geometric Analogy (GA) initially represented a solution in which geometric similarity between the real structural element (prototype) and the corresponding model (a reduced scale element) was compulsory. Thus, as is mentioned by the author of [13], this method can only be applied to some relatively simple cases. Other significant limitations of this method, compared to the future dimensional approaches analyzed, are summarized by the authors of [14].

The next step in this approach to prototype-model correlation was the Theory of Similarity (TS), which also requires geometric similarity; this is underlined by the authors of [15].

TS introduces the notion of the η scale factor, which is defined for each variable as a constant ratio as follows:

$$S_\eta = \frac{\eta_2}{\eta_1}, \quad (1)$$

where index 2 is used for model (η_2) and 1 is used for prototype (η_1).

Consequently, there are as many scale factors as there are variables that will describe the phenomenon, as illustrated by the author of [16].

The author of [17], based on a rigorous analysis, established that TS offers solutions for a few more cases because it involves functional similarity (i.e., it implies the existence of similar processes on the model and on the prototype at homologous points at homologous times).

To analyze high-complexity phenomena, Buckingham established Buckingham's π theorem [18].

The author of [19] provides the appropriate mathematical foundations, and thus, this theorem has become a useful tool in engineering.

This method, based on Buckingham's π theorem and perfected by specialists, will hereinafter be referred to as Classical Dimensional Analysis (CDA).

The author of [20] conducted a detailed analysis on the efficiency of implementing CDA in design, emphasizing the significance of this approach.

In [21], the authors provide a detailed analysis of the conceptualization of CDA, illustrating the method by presenting a number of software applications that can be employed in the modelling of various phenomena.

To extend the application of CDA to engineering problems, in [22], the author provides more information that is useful to specialists, showing that CDA can represent an effective means of addressing multiple technical problems.

Next, we present several ways in which CDA has been applied in various fields, highlighting the difficulties related to obtaining the dimensionless variables necessary to establish correlations between the prototype and the attached model.

In [23], the authors present useful experimental results regarding the convective heat transfer coefficient and pressure drop values obtained during CO_2 condensation and evaporation, taking into account different operating conditions in relation to the flow rate in micro-pipes. Through CDA, the authors established useful correlations between the Nusselt number and pressure drops. The dimensional correlations obtained can be applied in the calculation of pressure drops and heat transfer coefficients, both in mini-tubes and micro-tubes. The authors of [24] propose an effective combination of CDA and modern statistical design. They suggest that their approach is employed in hydrodynamic experiments, where there are a very large number of variables. They used the proposed method to evaluate the thrust of a propeller under several working conditions. The final propeller model was in good agreement with the test results. In [25], the authors analyzed the interaction of thermal radiation with particle-charged turbulence. In their analysis of this complex phenomenon, they addressed the advantages of CDA, although there were some limitations to the classical approach; these included the fact that it does not provide a unique set of necessary dimensionless variables and provides no solid support when obtaining the relative weight between the variables via measurements. The authors therefore propose a semi-empirical dimensional approach to solving the multi-physics turbulent flow problem, in terms of obtaining the dimensionless groups necessary for the phenomenon of particle-charged irradiated turbulence. The results obtained are very promising. The authors of [26] propose a useful approach to determining the energy absorption characteristics of a circular tubular structural element made from different materials. Based on several experimental tests, they developed a suitable FEM model of the energy absorption phenomenon. The authors applied CDA to obtain the model law required to describe the correlations between the displacements (caused by the produced deformations), the energy absorption, and the average crushing load of the analyzed tubes and the impact parameters, namely mass, velocity, etc. The model law obtained was in good agreement with the experimental results. Based on these results, they propose an efficient method for the appropriate lightweight design of these tubes.

In essence, CDA develops a finite number of π_j, j = 1, . . ., n dimensionless variables related to the real set of variables that govern the analyzed phenomenon. This set of dimensionless variables, representing the so-called ML, can predict the behavior of the prototype based on the experimental results of the model.

To deduce the ML of the CDA, which is described in detail in numerous references, there are, in principle, three main procedures; these are detailed by the author of [27] and include the following:

- Buckingham's π theorem;
- The partial differential equation is related to the corresponding analytical relationships;
- The grouping of the involved variables into dimensionless forms from the most straightforward equation (equations) related to the phenomenon.

Taking into consideration the abovementioned means of deducing the ML of CDA, it is clear that the CDA does not represent a user-friendly method, mainly due to the following shortcomings:

- It is a relatively chaotic procedure in identifying the π_j, j = 1, . . ., n dimensionless variables;
- It is not a reliable, easy, or unique means of obtaining the ML demanded;
- Its results depend on the ingenuity and previous experience of the specialist involved;
- It requires a solid knowledge of both higher mathematics and the phenomenon being analyzed;
- Due to the difficulties associated with its application, it is not a valuable tool for general engineers and researchers;
- One can only obtain the complete ML in some limited and special/particular cases;
- Its protocol does not allow a flexible prototype–model correlation in order to adapt the most suitable model, which will be involved in experimental investigations.
- These shortcomings are detailed and analyzed by the author of [1].

To optimize the dimensional approach and obtain the most suitable method, in [1], Szirtes successfully developed Modern Dimensional Analysis (MDA). MDA practically eliminates all the aforementioned shortcomings of CDA and provides engineers and researchers with a reliable and user-friendly tool, as analyzed in the following section.

3. Modern Dimensional Analysis (MDA)

3.1. The Principle of MDA

It should be noted that compared to CDA, in MDA, the constitutive relations of the model law do not represent, in the classical sense, the calculation relations of the phenomenon studied but only a few useful correlations between the variables that influence this phenomenon; more precisely, this is between the scale factors corresponding to the variables involved.

Consequently, these correlations, which constitute firm links between the scale factors of the variables involved in describing the phenomenon, should not be compared with analytical relations related to the phenomenon.

The deduction of these correlations, namely the elements of the model law, is facilitated by the unique and simple protocol elaborated by the author of [1]. The methodology, as presented below, is available to any specialist or engineer who wishes to implement useful prototype–model correlations in their research and development work.

Dimensional Modelling is based on MDA; it primarily aims to ensure that trials/tests are carried out on models (reduced or enlarged) to scale and that the results obtained are extrapolated to the prototype.

To achieve effective modelling, it is necessary to understand the basic physical phenomenon and include all relevant quantities (variables, parameters, and constants) in its description.

However, when comparing both theoretical approaches and classical dimensional methods, it is not necessary to know how these relevant quantities influence the phenomenon as a whole; this is perhaps the greatest advantage of Dimensional Modelling.

Within Dimensional Modelling, it is desirable to analyze/compare homologous phenomena that appear at homologous times, i.e., those that present positions, shapes, deformations, etc., at homologous times.

Dimensional Similarity is the cornerstone of Dimensional Modelling. The behavior of a system is defined by the set of dimensionless variables, which is established based on the relevant independent variables.

Thus, the two systems will be dimensionally similar if these corresponding dimensionless variables, row by row, assume identical values in the two systems. Therefore, the measurement results obtained by one system can be transferred to the other system, which is the essence of Dimensional Modelling.

Within Dimensional Modelling, the physical variables and constants involved can be divided into three distinct categories, as follows:

- Category I, where the sizes are freely chosen, i.e., the size is known in advance (where the sizes are given a priori or are chosen or calculated before starting the modelling process);
- Category II, where the sizes are obtained by applying the model law, respectively;
- Category III, where dimensions are obtained via actual measurements on the model.

If a quantity is obtained through a measurement on the prototype, this is Category I, because this measurement is independent of the actual modelling process.

The principle of MDA consists of the main steps below; from these, one can understand its utility.

First, the researcher selects all the variables that could have a particular influence on the given phenomenon, together with their dimensions. Due to the facilities of MDA, those variables that have an insignificant influence will be automatically eliminated during the calculi imposed by the unique protocol conceived by the author of [1].

From these variables, one has to choose a few numbers directly related to the forthcoming experimental investigations on the attached model. It will constitute a quadratic matrix A from the exponents of the involved (above selected) variables, with a single condition: $\det|A| \neq 0$, where matrix A is invertible. These variables, denoted as independent variables, allow their magnitudes to be freely chosen a priori for both prototype and model; this represents an incontestable advantage of MDA compared to CDA, TS, and GA. These advantages will be analyzed in the following section. The dimensions of the independent variables are denoted as primary dimensions; their exponents constitute the elements of matrices A and B, which are also analyzed in the following section.

The exponents of the remaining n variable, which are expressed as functions of the primary dimensions, denoted as dependent variables, will constitute the matrix B, where one can find (can be accepted) variables with the same dimensions (there are not any condition for matrix B to be quadratic as well as invertible). These dependent variables can be chosen a priori as dimensions only for the prototype; for the model, their dimensions will exclusively result from the rigorous application of the inferred ML.

In addition, in matrix B, among the n dependent variables mentioned, there are also several variables that belong to the prototype whose experimental determination is complicated, either because of the high cost involved, or because of the extremely

difficult/complex conditions of their experimental investigation; determining their size is, in fact, the main purpose of the dimensional analysis that is performed.

In these cases, the size of the dependent variables of the required prototype is given a priori for the attached model only; for the prototype, their sizes will result exclusively from the application of the ML, based on the experimental investigations performed on the model.

Based on these two B and A matrices, completed with a $D \equiv I_{n\times n}$ unite matrix of the order n, with the special $C = -(A^{-1}\cdot B)^T$ matrix, one will obtain the so-called Dimensional Set (see Tables 1 and 2).

Table 1. The Dimensional Set [1].

One has k primary dimensions	1. 2. 3. ... k.	B	A
One has n dependent variables in matrix B and the same resulting number of π_j, dimensionless quantities	1. 2. 3. ... n	$D \equiv I_{n\times n}$	$C = -(A^{-1}\cdot B)^T$

Table 2. The Dimensional Set for a given case.

	Dimensions	K_1	K_2	K_3	K_4	K_5	K_6	K_7	K_8	K_9	K_{10}	
B	r_1											A
	r_2											
	r_3											
	r_4											
D	π_1	1	0	0	0	0	0					C
	π_2	0	1	0	0	0	0					
	π_3	0	0	1	0	0	0	e_3	f_3	g_3	h_3	
	π_4	0	0	0	1	0	0					
	π_5	0	0	0	0	1	0					
	π_6	0	0	0	0	0	1					

Each line of the matrices D-C, which are interpreted/extracted based on the unique protocol conceived by the author of [1], will represent one element of the demanded ML.

In this sense, to illustrate this methodology, let us assume that ten $(K_1,\ K_2,\ \ldots,\ K_{10})$ variables have been identified for the phenomenon under analysis, of which four $(K_7,\ K_8,\ K_9,\ K_{10})$ are main variables with $(r_1,\ r_2,\ r_3,\ r_4)$ dimensions and $n = 6$ $(K_1,\ K_2,\ \ldots,\ K_6)$ dependent variables (see Table 2).

Matrix B is colored yellow, Matrix A is green, Matrix D is red, and Matrix C is purple. Useful notes

- If all $(e_1\ \ldots\ldots\ h_6)$ values are zero in the special matrix C, in the column of one of the $(K_7,\ K_8,\ K_9,\ K_{10})$ main variables, then that variable is insignificant for the analyzed phenomenon and must be replaced by another (so it is automatically eliminated from the set of variables initially chosen);
- An element of the complete ML, for example π_3, is obtained based on relation (2)

$$\pi_3 = (K_3)^1 \cdot (K_7)^{e_3} \cdot (K_8)^{f_3} \cdot (K_9)^{g_3} \cdot (K_{10})^{h_3} = 1, \tag{2}$$

where some of the $(e_3, \ldots, h_3)$ exponents can be positive, negative, or even zero, which is why the final expression of π_3 is a usual algebraic fraction.

- The following steps are then performed:
  - Replace the K variables with their S_K scale factors;
  - The scale factor of the demanded K_3 variable is expressed, i.e.,

$$S_{K_3} = \frac{1}{\left(S_{K_7}\right)^{e_3} \cdot \left(S_{K_8}\right)^{f_3} \cdot \left(S_{K_9}\right)^{g_3} \cdot \left(S_{K_{10}}\right)^{h_3}} = \frac{K_{3,2}}{K_{3,1}} \tag{3}$$

    where $K_{3,2}$ refers to the model and $K_{3,1}$ refers to the prototype, regarding the K_3 dependent variable.

  Depending on the type of this K_3 variable (whether it refers to the prototype or the model), one of the magnitudes is known (was chosen) a priori, and the other will result from this element of the ML.

  - By applying this protocol to all six $(K_1, K_2, \ldots, K_6)$ dependent variables, the full (complete) ML will be obtained; for the rest of the aforementioned dimensional methods, this can only be achieved in very particular cases.

3.2. The Main Advantages of MDA

The main advantages of MDA are as follows:

- Unlike GA, TS, and CDA, it does not require an in-depth knowledge of the field or higher mathematics. It only requires the consideration of variables (along with their sizes/dimensions), which may have an influence on the analyzed phenomenon;
- It has a unitary approach, which stands out for its simplicity, safety, and excellent flexibility, finally offering the complete ML. For the methods mentioned above (GA, TS, and CDA), this can only be achieved for some particular and relatively straightforward cases;
- Furthermore, from this complete set of MLs, particular cases of the analyzed phenomenon can be obtained without difficulty and assigned to the model that best fits the analyzed prototype;
- Its outstanding qualities are emphasized, as well as its ability to merge the initial variables, dividing them to obtain an optimal number of dimensionless variables (wanted to be minimal) to form the requested ML; these are very important features for the symmetric cross-sectional structural elements;
- Another advantage of MDA is its ability to establish new sets of variables from the general case, as follows:
- If a new setting for the independent variables is created, then it becomes possible to carry out another experimental strategy that is perhaps more appropriate for the new model;
- When a new selection of dependent variables is made, e.g., by eliminating some variables from this initial (entire/complete) set, the remaining ones will not be influenced; in other words, the expressions of a given set will not be influenced by the fact that some of the dependent variables are or are not taken into account;
- MDA provides more information during the definition of relevant variables, increasing the degree of freedom during the selection of model properties and thus enabling a more reliable description of the prototype.

If we consider that among the initial set of independent variables, there are the dimensions of the cross section of the analyzed structural element, considered rectangular with a, a', and b, geometric similarity is mandatory (see Figure 1 below).

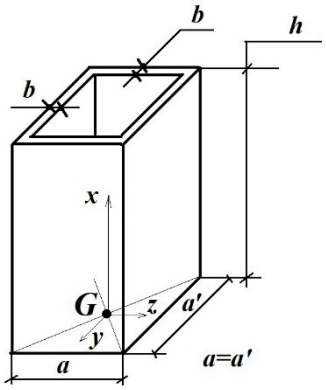

Figure 1. The main sizes of the tested elements, where L_z = a; L_y = a′ $\delta_y = L_y$; $\delta_z = L_z$ [28].

Instead of these sizes, a, a', and b, we propose introducing the I_{zG} second-order moment of inertia of the cross section. In this case, the aforementioned geometric similarity condition will disappear. Consequently, it becomes possible to attach a more suitable model to the prototype, which has another kind of cross section; this is because only the corresponding scale factor $S_{IzG} = I_{zG2}/I_{zG1}$, based on relation (1), has to remain constant; index 2 is related to the model, and index 1 is related to the prototype, respectively.

Similarly, if the E Young modulus is accepted as an independent variable, the model can be manufactured from a material that is different from the prototype.

By combining these last two, that is, merging them into the $E \cdot I_{zG}$ stiffness module, neither the shape of the cross section nor the material of the two elements (prototype and model) is subjected to any restriction; in addition, the geometric similarity, which always strongly constrains the attached model, is improved. These features are also important in structural elements with a symmetrical cross-section.

Regarding the challenges related to fire protection, it is well known that the ς shape factor is a significant variable; this is defined as the ratio of the cross-sectional A_{lat} lateral area and volume V, and is considered as a unitary $x = 1$ length of the structural element. This can be expressed as the ratio of the cross-sectional P perimeter and cross-sectional A_{tr} (transversal) area, as follows:

$$\varsigma = \frac{A_{lat}}{V} = \frac{P}{A_{tr}} \left[\frac{1}{m}\right] \quad (4)$$

If the ς shape factor is selected as the independent variable, there are more opportunities to obtain more general (generalizable) models in which the preservation of the geometric similarity is not mandatory; the model can have a different cross-sectional shape in order to provide a ς scale factor with a certain value/magnitude.

Similarly, the facilities and flexibilities of the attached model can be utilized by using the introduced Q heat, the corresponding $\dot{Q}$ heat flux (heat rate), and the imposed t or Δt thermal regime, which is analyzed below in Section 3.3.

3.3. Results of Obtaining the MDA Model Law

Given the theoretical approach of MDA described above, the authors of this study conducted detailed studies on the heat transfer of thermally unprotected steel structural members with a double symmetrical cross section subjected to a point heat source located at their base. The authors then obtained some useful MLs [28].

Based on careful analysis, the authors established the main variables that influence heat transfer in these uncovered (thermally unprotected) bars. Of these variables, only the following will be of interest for the present case: heat Q [J]; heat rate (heat flux) $\dot{Q} = \frac{dQ}{d\tau}$ [W]; time τ [s]; thermal conductivity (steel) along direction x, λx [W/(m °C)]; the cross-sectional

area of bar Atr [m^2]; the bar's dimensions Lx, Ly, Lz [m]; the shape factor ς [1/m]; and the temperature variation ΔT [K] or Δt [°C].

In addition, it should be mentioned that in the case of classical dimensional approaches (GA, TS, and CDA), both of these variables and the derived (inferred/obtained) dimensionless variables are directly related to physical phenomena and have a certain physical meaning/significance.

To deduce the model law required, either the standard rectangular section with a $\neq$ a$'$ or its special case can be considered, i.e., the square section a = a$'$; both of these are double symmetrical cross-sectional structures (see Figure 1). Dimensions of the tested elements with different scales are presented in Table 3.

Table 3. Dimensions of the tested elements, with different scales [28].

Dimensions of the Tested Elements, Having			
[mm]	**Scales**		
	1:1	1:2	1:4
$a = a'$	350	175	87.5
b	16	8	4
$h = L_x$	400	200	100

Consequently, the complete set of selected variables is

$(Q,\ \dot{Q},\ L_z,\ \Delta t,\ \tau,\ \lambda_{x\ steel},\ \varsigma,\ A_{tr},\ L_x,\ L_y,\ \delta_{y\ steel},\ \delta_{z\ steel},\ t^*)$, where t^* represents the required temperature along one of the structural elements, as will be seen below.

In the current case, we selected two variants of independent variables, which constitute the elements of the corresponding matrix A

I. $(Q,\ L_z\ ,\ \Delta t,\ \tau,\ \lambda_{x\ steel},\ \varsigma)$, II. $(\dot{Q},\ L_z\ ,\ \Delta t,\ \tau,\ \lambda_{x\ steel},\ \varsigma)$.

From this set, except for Q and $\dot{Q}$, which are part of the set of independent variables, i.e., they form matrix A, the rest of the variables form matrix B, i.e., $(\dot{Q},\ A_{tr},\ L_x,\ L_y,\ \delta_{y\ steel},\ \delta_{z\ steel},\ t^*)$ and

$(Q,\ A_{tr},\ L_x,\ L_y,\ \delta_{y\ steel},\ \delta_{z\ steel},\ t^*)$, respectively.

To show that the objective of this study was achieved, let us focus on one of these sets, namely, on variant I, where matrix B will be $(\dot{Q},\ A_{tr},\ L_x,\ L_y,\ \delta_{y\ steel},\ \delta_{z\ steel},\ t^*)$, and the Dimensional Set obtained will ultimately be the one presented in Table 4. It should be emphasized that to obtain an optimal ML, the length on the x, y, and z axes was divided, namely the length m was split/divided [1].

Table 4. The Dimensional Set obtained.

	$\dot{Q}$	A_{tr}	L_x	L_y	$\delta_{y\ steel}$	$\delta_{z\ steel}$	t^*	Q	L_z	Δt	τ	$\lambda_{x\ steel}$	ς
m_x	2	0	1	0	0	0	0	2	0	0	0	1	0
m_y	0	1	0	1	1	0	0	0	0	0	0	0	−1
m_z	0	1	0	0	0	1	0	0	1	0	0	0	0
kg	1	0	0	0	0	0	0	1	0	0	0	1	0
s	−3	0	0	0	0	0	0	−2	0	0	1	−3	0
°C	0	0	0	0	0	0	1	0	0	1	0	−1	0
π_1	1	0	0	0	0	0	0	−1	0	0	1	0	0
π_2	0	1	0	0	0	0	0	0	−1	0	0	0	1
π_3	0	0	1	0	0	0	0	−1	0	1	1	1	0
π_4	0	0	0	1	0	0	0	0	0	0	0	0	1

Table 4. *Cont.*

	$\dot{Q}$	A_{tr}	L_x	L_y	$\delta_{y\ steel}$	$\delta_{z\ steel}$	t^*	Q	L_z	Δt	τ	$\lambda_{x\ steel}$	ς
π_5	0	0	0	0	1	0	0	0	0	0	0	0	1
π_6	0	0	0	0	0	1	0	0	−1	0	0	0	0
π_7	0	0	0	0	0	0	1	0	0	−1	0	0	0

Based on the protocol described in Section 3.1, with the help of relations (2) and (3), we obtained the model law, i.e., relations (5)–(11).

$$\pi_1 = \dot{Q} \cdot Q^{-1} \cdot L_z^0 \cdot \Delta t^0 \cdot \tau^1 \cdot \lambda_{x\ ot}^0 \cdot \varsigma^0 = \frac{\dot{Q} \cdot \tau}{Q} = 1 \Rightarrow \frac{S_{\dot{Q}} \cdot S_\tau}{S_Q} = 1 \Rightarrow S_{\dot{Q}} = \frac{S_Q}{S_\tau} \quad (5)$$

$$\pi_2 : S_{A_{tr}} = \frac{S_{L_z}}{S_\varsigma} \quad (6)$$

$$\pi_3 : S_{L_x} = \frac{S_Q}{S_{\Delta t} \cdot S_\tau \cdot S_{\lambda_{x\ steel}}} \quad (7)$$

$$\pi_4 : S_{L_y} = \frac{1}{S_\varsigma} \quad (8)$$

$$\pi_5 : S_{\delta_{y\ steel}} = \frac{1}{S_\varsigma} \quad (9)$$

$$\pi_6 : S_{\delta_{z\ steel}} = S_{L_z} \quad (10)$$

$$\pi_7 : S_{t^*} = S_{\Delta t} \quad (11)$$

Through a careful analysis of the two sets of independent variables proposed, their efficiency can be ascertained in terms of their capacity to attach models that are as flexible as possible and affordable.

In the following, let us summarize the main advantages of the set of variables analyzed.

- The heating of the lower end of the tested structural element is easily controlled and repeatable via Q heat or the associated $\dot{Q}$ heat rate. The independent variables chosen in the analyzed variants I ensure, among other things, that the prototype and model of thermal regimes, lengths, scale factors, and materials are chosen independently. This ultimately led to the attainment of very flexible and advantageous attached models.
- Thus, by choosing Q or Δt a priori independently for the prototype and the model, we will be able to perform experiments in comfortable and advantageous conditions. Thus, if we choose a Q or Δt that leads to a thermal regime in the order of 900 °C for the prototype, we will be able to choose a thermal regime that leads to temperatures in the order of 500 °C for the model, as we will see in Section 5.3.
- Similarly, the (chosen) exposure time τ imposed a priori upon heating will provide similar benefits.
- Using length L_z as an independent variable will allow us to assume the same scale factor for all dimensions of the structural elements subjected to the tests, or only for this one. Thus, if we want different scale factors for the dimensions L_x and L_y, and the thicknesses $\delta_{y\ steel}$ and $\delta_{z\ steel}$, the model law will allow us to achieve this, in strict compliance with the elements of the model law related to these dimensions.
- It can also be observed that because relations (8) and (9) are similar, we will have the same scale factors for L_y and $\delta_{y\ steel}$. In addition, relations (7) and (8) allow us, if desired, to apply this set of model laws to rectangular or square sections, with equal wall thicknesses ($\delta_{y\ steel} = \delta_{z\ steel}$); if necessary, they also allow us to choose different

wall thicknesses along the two z and y directions. If we adopt a single scale factor according to L_z for all lengths/dimensions involved, then relations (6)–(9) can simply be ignored.

- Including t^* in the set of dependent variables helps solve two major problems:
  - If we have performed the set of experiments on a certain model at a certain temperature, based on the scale factor $S_{\Delta t}$ and using relation (11), we will then be able to forecast all temperatures of the prototype at its homologous points with the model based on the results obtained by the model; this is illustrated later in Section 5.3.
  - If we have performed tests at a certain thermal regime on the model of a spatial structure, then the forecast of the thermal fields/regimes related to the prototype (untested!) at the level of all homologous points, corresponding to a thermal regime chosen a priori, will become possible again if relation (11) is used; this is detailed in the same Section 5.3.

4. Premises Regarding Analytical Calculations and Experimental Investigations

It should be noted from the outset that all theoretical (analytical and numerical) and experimental investigations have considered the case of steel structural elements heated at their base by point sources. This case corresponds to the context of fire, when this structural element, i.e., the column of industrial or residential buildings, is located either one floor above the actual fire source, or when the fire source is located right at the base of the column.

For all these investigations, the authors of this study used a series of rigorously theoretically verified and experimentally validated data as their starting point; these are analyzed below.

(a) The author of [29] demonstrated that the heat distribution law (as well as the temperature's one) for solid cross-sectional straight bars (for the whole its x = L_x = h length) in the m = const hypothesis, i.e., heated at its lower end, is described by the following:

$$t(x) = c_1 \cdot e^{m \cdot x} + c_2 \cdot e^{-m \cdot x} \tag{12}$$

In Equation (12), the notations are as follows:

- c_1 and c_2 are constants for the $x = 0$ and $x = L_x$ boundary conditions;
- $t(x)$ is the temperature of the bar at level x from the heated end (its lower end);
- m is a generally accepted parameter, which is calculated as follows:

$$\mathrm{m} = \sqrt{\frac{P \cdot \alpha_n}{A \cdot \lambda}} \left[\frac{1}{m}\right] \tag{13}$$

where α_n is the heat transfer coefficient of the bar's nappe.

In the m = const hypothesis, the heat transfer coefficient and thermal conductivity will also be considered constants along the bar. In addition, the ambient temperature is considered constant along the bar. Considering m = const, Equation (13) can be used to obtain a beneficial and practical relationship for $\alpha_n(x)$ through experimental measurements, i.e.,

$$\alpha_n(x) = m^2 \cdot \frac{A}{P} \cdot \lambda(x) \tag{14}$$

(b) In [30], the authors, through high-precision experimental investigations, demonstrated that in the case of bars with a tubular cross section, relation (12) is only applicable

to some well-defined portions; it is recommended that the tubular bar is divided into (minimum) three parts, i.e., L_I = (0, . . ., 0.06) L_x; L_{II} = (0.06, . . ., 0.12) L_x; and L_{III} = (0.12, . . ., 1.0) L_x, with their own m = const. Both the corresponding values of m and the temperature distribution laws must be established through high-precision experiments.

(c) The author of [31] performed a series of meticulous tests to further expand the research on heat transfer and thermally protected steel double symmetrical cross-sectional structural elements (for example, with intumescent paints). The purpose of these tests was to determine the influence of the direction of the introduction of heat flow into the thermally protected structural element on the λ thermal conductivity coefficient of the thermal protective layer.

At present, fire resistance tests, especially in the case of full-scale structural elements, are usually carried out in specially designed furnaces or special chambers, whose cost is significantly increasing. In addition, it is unclear whether these tests can be repeated.

If an electric heating system could be used (direct heating of the steel structural element) instead of these furnaces or specially arranged spaces, the cost would decrease, and the repeatability of the experiments would be ensured. That is why the author of [31] performed detailed tests on the change in the thermal conductivity coefficient of the thermal protective layer with the change in the direction of heat flow introduction.

The reference set was a classical furnace in which heat flow was introduced from the outside. Compared to it, the second set of experiments used an original electric bench, which directly heated the steel structural element tested.

By comparing the results of these two sets of measurements, it could be established that the heating direction of the thermally protected structural element does not influence the magnitude of the thermal conductivity coefficient λ, as found by the author of [31], i.e.,

λ = 0.11021 W/(m °C) (for heating inside),

λ = 0.1089 W/(m °C) (for heating from outside), with less than 1% deviation.

Consequently, inverse heating (from the inside) will be more favorable, involving only some simple and inexpensive electrical resources instead of huge ovens.

To satisfy these aspects, the authors developed an original electric stand, capable of testing both prototypes and attached models from the point of view of heat transfer. All these facilities and performances of this stand (test bench) are presented in the paper [32].

5. Results Obtained for Structural Elements with a Double Symmetrical Cross Section

5.1. Experimental Results on Prototype and Attached Models, Corresponding to the Column Segment

To validate the MLs detailed in [28], the authors used the abovementioned original electrically heated test bench, which not only ensures high-precision heating and the repeatability of the experimental investigations performed, but also provides an easy-to-use and safe investigation modality.

Based on the results of [30], detailed in Section 4, it is worth noting that in the experimental investigations of the prototype and the models made at scales of 1:2 and 1:4, according to Figure 1, only the L_I zone was modelled/analyzed practically; here, the thermal gradient was at its maximum. In these cases, considering that the real length of the column/column is L_x = 5 m, this L_I portion is only L_I = 0.30 m. Consequently, only the last two thermal resistances are disposed/mounted in the L_{II} zone/interval.

In the case analyzed by the authors of [28], where the model related to the entire column (also having double symmetric cross sections) was studied, i.e., the model was made/manufactured at a scale of 1:10, all three intervals were followed.

To monitor the temperature, the authors used some PT 100-402 (Jumo, RS Components Ltd., Birchington Road, Corby, Northants, NN17 9RS, UK) thermal resistances, which were fixed with M3 screws at the mentioned levels (Figure 1).

For structural elements with a symmetrical cross section, higher-precision assessment is advantageous due to the fact that we can obtain more identical measurement points. From these, a more accurate average value can be obtained; this is compared to the values obtained from elements with an asymmetrical cross section.

To achieve a stabilized thermal regime, at the last level of thermal resistance, the measured temperatures have a maximum oscillation of (0.2, . . ., 0.3) °C for 120 s.

As mentioned previously, the experimental investigations involved not only the segment of the initial structural element (a real column segment) but also the scale models attached under the same testing conditions.

Considering the role of the respective element, we directly obtained measured and calculated reference data from it.

The abovementioned and inferred MLs (for a detailed analysis, see [28]) were finally successfully validated based on multiple experimental investigations. In this regard, the structural element was either a prototype or a model in different scenarios. Thus, multiple and high-accuracy validation of the conceived MLs became possible.

Finally, for Q and their scale factors, a perfect correspondence was found, while for the rest of the variables, this was with errors of at most 2.5%. Thus, both the deduced MLs and the efficiency of their original electric test bench could be considered adequate for future theoretical-experimental investigations.

This set of measurements (monitoring thermal fields along the structural elements according to Figure 1) is detailed in the following:

Based on the data from Figure 1, the coordinates of the thermal resistances can be obtained (see Table 5). To perform a comparative analysis, the authors introduced the L_Ψ [%] conventional length, representing a percentage of the whole length of the tested structural element. Table 6 summarizes the conventional and real lengths of the tested elements, as well as the location of the thermal resistances.

Table 5. The mounted thermal resistance coordinates [28].

Prototype, at Scale 1:1	**Model I., at Scale 1:2**	**Model II., at Scale 1:4**
Coordinates $x(j)$ [mm]		
0	0	0
20	20	20
110	60	55
200	105	90
290	150	
380	190	

Table 6. The conventional and real lengths of the tested elements and the position of the thermal resistances.

Conventional Length	**Real Length [mm]**			**Coordinate of Thermal Resistances [mm]**		
L_Ψ [%]	Prototype	Model I (1:2)	Model II (1:4)	Prototype	Model I (1:2)	Model II (1:4)
0	0.00	0.00	0	0	0	0
2.5 *	10.00	5.00	2.5	10 *	5	2.5

Table 6. *Cont.*

Conventional Length	Real Length [mm]			Coordinate of Thermal Resistances [mm]		
5 *	20.00	10.00	5	20 *	10	5
10 **	40.00	20.00	10	40	20 **	10
20 ***	80.00	40.00	20	80	40	20 ***
27.5 *	110.00	55.00	27.5	110 *	55	27.5
30 **	120.00	60.00	30	120	60 **	30
37.5	150.00	75.00	37.5	150	75	37.5
50 *	200.00	100.00	50	200 *	100	50
52.5 **	210.00	105.00	52.5	210	105 **	52.5
55 ***	220.00	110.00	55	220	110	55 ***
72.5 *	290.00	145.00	75	290 *	145	75
75 **	300.00	150.00	72.5	300	150 **	72.5
90 ***	360.00	180.00	90	360	180	90 ***
95 *	380.00	190.00	95	380 *	190	95

Note: The positioning of the involved thermal resistances corresponds to *—the prototype; **—Model I; ***—Model II. These notations remain valid in the following tables.

Based on the temperature measurements performed and the predicted values obtained with the curve fitting methods, which were used to determine the intermediate points between the actual measurement points, the subsequent drawing of comparative thermal curves is ensured, i.e., at the homologous points of these tested elements.

These increasing temperatures were only chosen to demonstrate that as the temperature increases, the obtained curves will move closer and closer; from 500 °C, these curves can be considered to overlap.

In order to provide a general overview, the authors proposed the introduction of a relative T_Ψ [%] temperature, representing the percentage of temperature remaining from the nominal To,n [°C] temperature, which was monitored and imposed at the base of the electric heated structural element [28]. Using this new $T_\Psi - L_\Psi$ system of coordinates, the results are synthesized in Figures 2–4.

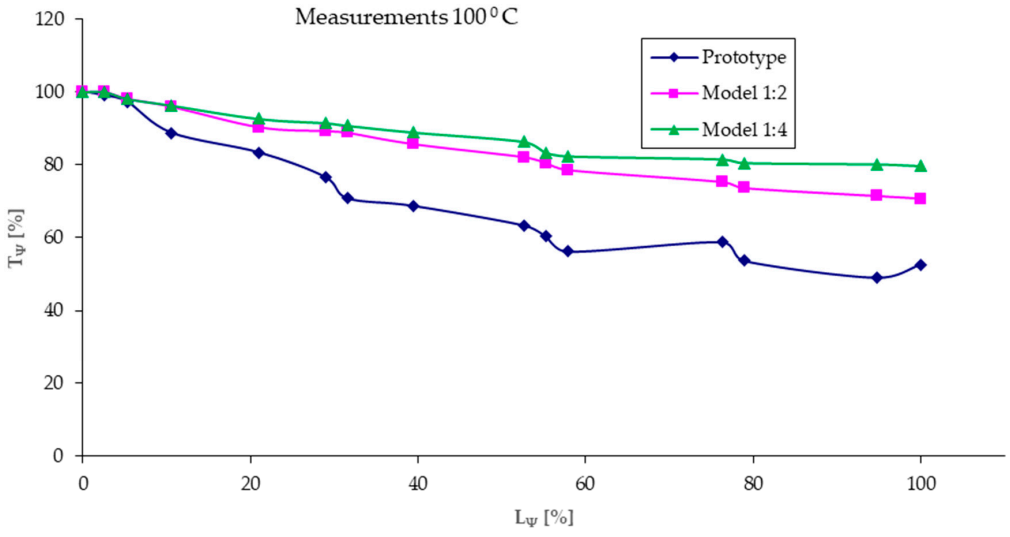

Figure 2. The comparative results of the values measured at $T_{O,n} = 100$ °C in real points, as well as those in the homogenous points, obtained by curve fitting in $T_\Psi - L_\Psi$ coordinates.

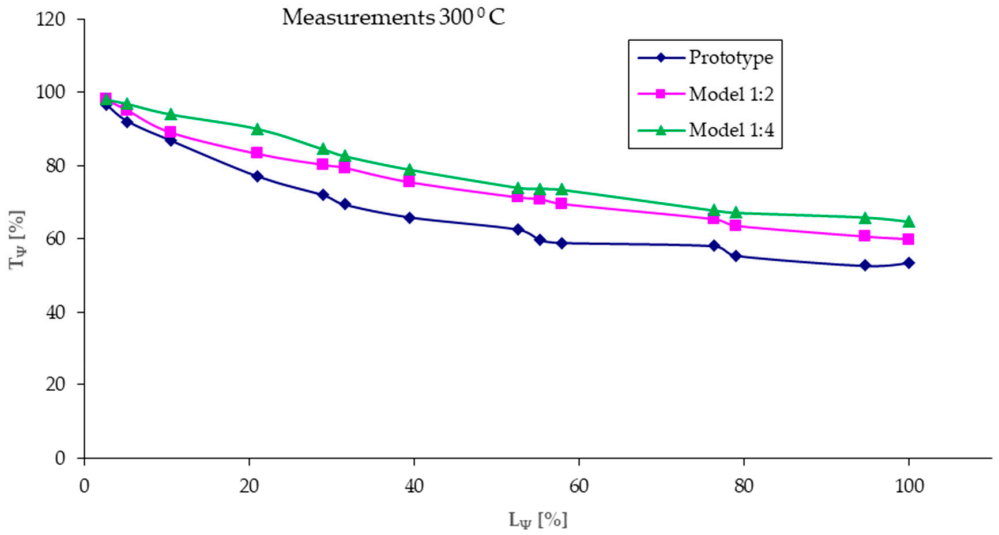

Figure 3. The comparative results of the values measured at $T_{O,n} = 300$ °C in real points, as well as those in the homogenous points, obtained by curve fitting in $T_\Psi - L_\Psi$ coordinates.

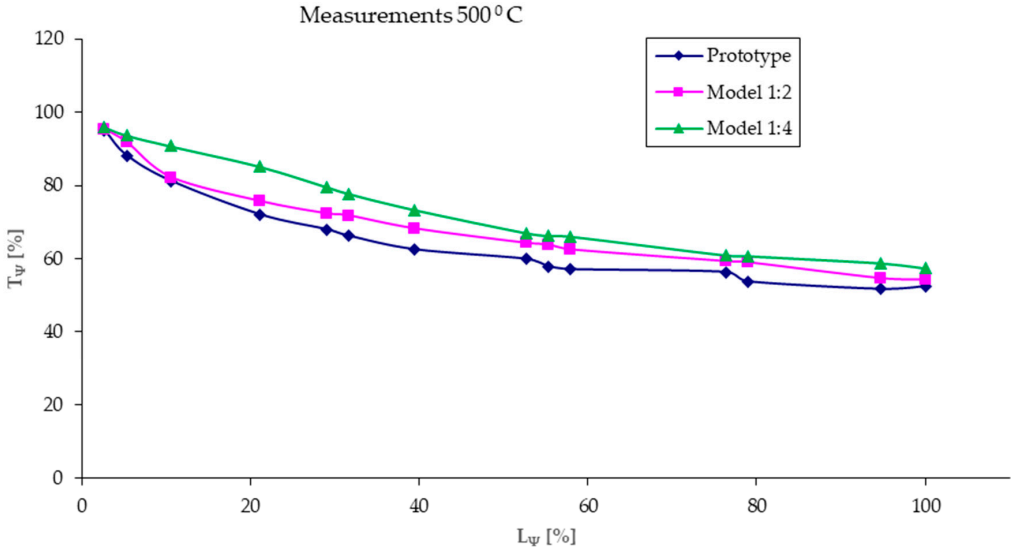

Figure 4. The comparative results of the values measured at $T_{O,n} = 500$ °C in real points, as well as those in the homogenous points, obtained by curve fitting in $T_\Psi - L_\Psi$ coordinates.

From a careful analysis of Figures 2–4, one can observe the correspondence/better approximation of the measured values when the arrangement of thermal resistances coincided or occupied closer positions on both the structural elements tested. When using forecast values obtained via curve-fitting methods, differences became increasingly insignificant as the temperature increased.

If we carefully analyze the diagrams in Figures 2–4, it can be seen that as the temperature increases, the differences between the curves of the three cases (prototype and the two models) decrease. In addition, considering real fire cases, where temperatures are well above 500 °C, it can be stated that these practical conventional curves will overlap, which will allow for a much easier analysis of the prototype-model correlation.

Based on a careful analysis of the results provided in Figures 2–4, the following essential elements for the further application of MDA can be noted:

- As the temperature increases, the differences between the temperatures of the homologous points in the prototype and the two models decrease.

- Regardless of whether we obtained real measurement points or forecasts through curve fitting, these differences decreased with an increase in temperature.
- The similar behavior of the homologous points related to the three tested structural elements with a double symmetrical cross section, especially at high temperatures (as in the case of fires), confirms the e validity of the functional similarity mentioned in Section 2.
- Consequently, this functional similarity can inevitably be extended to the rest of the elements of the analyzed structure, with the validity of the ML deduced for these analyzed structural elements subjected to heating tests.

5.2. Numerical Results on Prototype and Attached Models, Corresponding to the Column Segment

To perform the numerical modelling that is necessary for future fire simulation strategies, the authors performed a numerical analysis of the column/column segment and the models attached to it.

The authors used the ANSYS 2023 R1 version commercial software package for numerical simulation to determine the temperature distribution in rectangular steel structures (prototype and Models I and II). The program provides several options for thermal conductivity analysis, including a steady-state thermal analysis based on the finite element method used in the mechanical environment.

The 3D geometries used for numerical simulations were prepared based on the existing data. To ensure a good result, it is essential to create a suitable numerical mesh. During meshing, the optimal number of cells must be found; this is because the speed and accuracy of the calculation depend significantly on the composition, design, and number of mesh elements created.

Of course, for structural elements with a symmetrical cross section, the required size of the half band (half strip) can be reduced, along with the computational speed.

The use of more element numbers results in higher accuracy; however, the computational time will also increase, as will the memory requirements of the computer. Therefore, a mesh independence test was carried out; three different meshes were created on the prototype with element numbers G1 = 42,107, G2 = 117,386, and G3 = 667,768. In all three cases, hexahedral cells were used. During the test, the steel double symmetrical cross-section structure was heated to 500 °C. The temperature distribution along the length of the structure was investigated, and it was found that the difference between the G1 and G3 types of netting is less than 0.1%. The G3 mesh consists of a large number of elements, and in the future, we also want to analyze higher temperatures and thus use the G2 mesh for further tests. The number of elements on the prototype (1:1 scale) is 117,386, while Model I (1:2 scale) and Model II. (1:4 scales) consist of 130,482 and 159,570 elements, respectively.

The results of the measurements and calculations are compared; the measurement results are denoted by EM = Experimental Measurement, while the numerical values are denoted by FEM = Finite Element Method. In this regard, the diagrams of the obtained experimental results were superimposed onto the corresponding FEM simulation results (see Figures 5–7).

It can be seen that as the temperature increases, the differences between the curves of the three cases (prototype and the two models) decrease. In addition, considering real cases of fire in which temperatures are much higher, it can be stated that these practical conventional curves will overlap, enabling a much simpler analysis of the prototype–model correlation.

In the careful analysis of these diagrams, it must also be taken into account that in numerical simulation, modelling the temperature stabilization state is complicated. In this regard, dividing the heated tubular bar into at least three L_I, L_{II}, and L_{III} intervals with

individual heat transfer laws, evidenced by meticulous experimental measurements, is currently not possible in numerical modelling. For this, it would be necessary to carry out detailed preliminary experimental measurements on different types of tubular bars, from which the probable heat transfer laws can be deduced and which will later be introduced into the numerical modelling protocols.

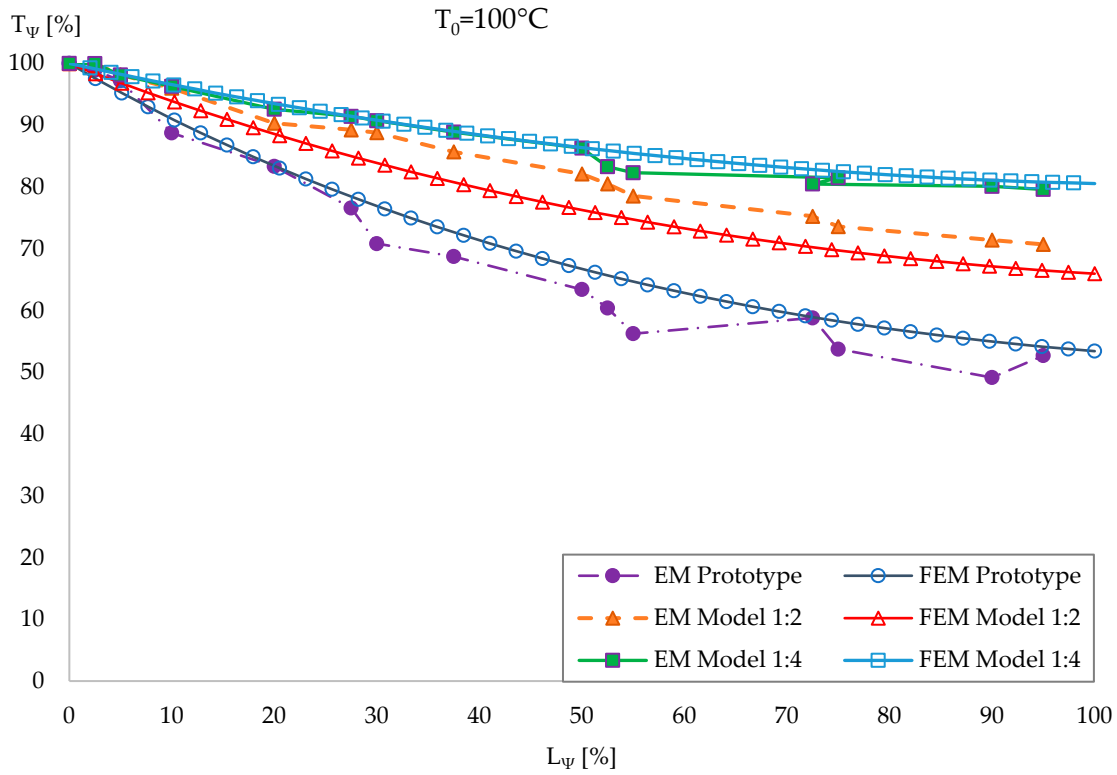

Figure 5. Experimental and numerical results at T_0 = 100 °C in $T_\Psi - L_\Psi$ coordinates.

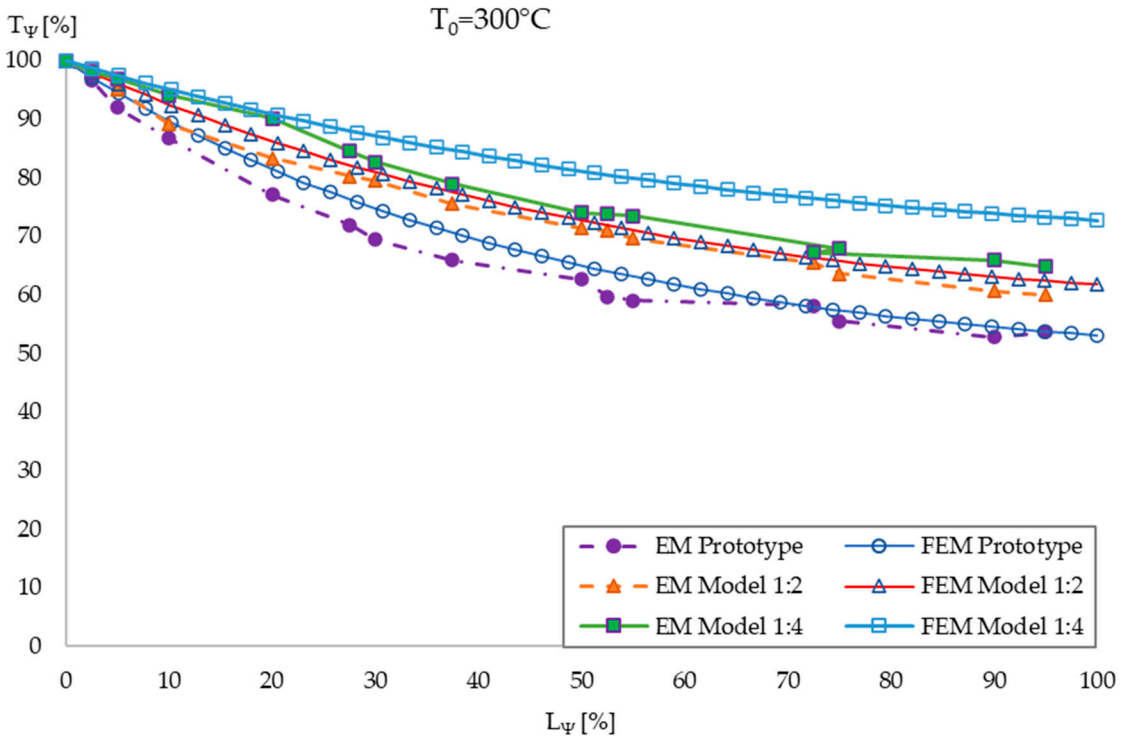

Figure 6. Experimental and numerical results at T_0 = 300 °C in $T_\Psi - L_\Psi$ coordinates.

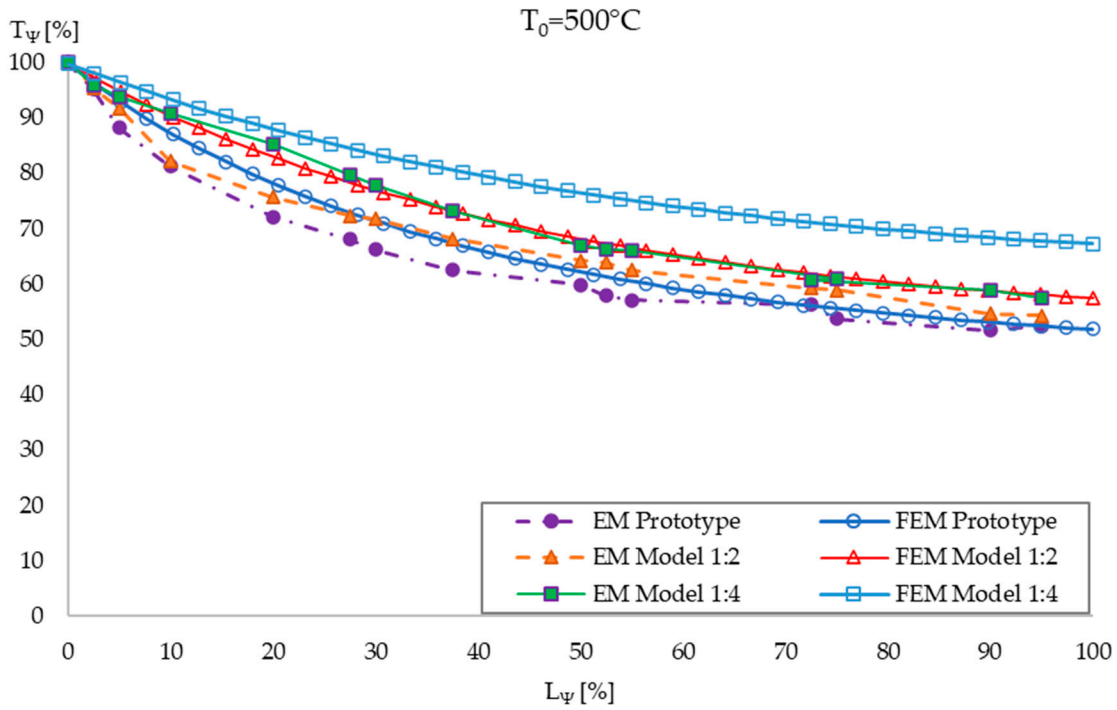

Figure 7. Experimental and numerical results at T_0 = 500 °C in $T_\Psi - L_\Psi$ coordinates.

Thus, in ordinary cases, it is only possible to pass a heat flow and reach the base of the structural element of the imposed nominal temperature. In the case of the actual measurements, however, those thermal values were monitored, corresponding to the imposed stabilized state, as stated before.

5.3. Experimental Results on Homologous Points of the Prototype and Attached Models, as Well as the Real Structure

In Section 3.3, when determining the model law, it was shown that in the Dimensional Set, among the dependent variables, the temperature t* was also included.

The purpose of this variable was twofold.

- Based on the results of measurements performed on the model, it was able to forecast the thermal field at the prototype, which was only evident at its homologous points with the model.
- Based on experimental measurements on the model of a spatial structure, it makes it possible to forecast temperatures on the original spatial structure, i.e., on the prototype.
- In these calculations, the $S_{\Delta t}$ scale factor relation (11) can be used in an explicit form.

$$S_{t^*} = S_{\Delta t} \Leftrightarrow \frac{t_2^*}{t_1^*} = \frac{T_{02}}{T_{01}} \tag{15}$$

where T_{02} and T_{01} represent the a priori accepted temperatures for the model and prototype, respectively (before the start of the experimental measurement on the model), and t_2^* and t_1^* represent the actual temperature measured on the model and the required temperature on the prototype, respectively, at their homologous points.

t_1^* is expressed in relation (15), and the final calculation relation (16) is obtained.

$$t_1^* = \frac{T_{01}}{T_{02}} \cdot t_2^* \quad \text{or} \quad t_1^* = \frac{t_2^*}{S_{\Delta t}} \tag{16}$$

This relation (16) will be applied to all homologous points of the prototype and model.

It should be noted that through this single dependent variable t^* [°C], we will be able to correlate the homologous points of the model (whether it is a single element or a scale modelled structure) with those of the prototype.

Relation (16) can be applied along the three coordinate directions/axes, i.e., for the quantities t_x, t_y, and t_z, as will be shown below.

In conclusion, the proposed set of experimental investigations is carried out exclusively on the model. By substituting in the corresponding/adequate elements of the *ML*, the temperatures $t_{x,2}$, $t_{y,2}$, $t_{z,2}$ obtained from measurements (related to the model) and the probable temperatures $t_{x,1}$, $t_{y,1}$, $t_{z,1}$ of the prototype in these areas can be obtained by applying relation (16).

To illustrate this feature, we will use the results of experimental measurements on a column model of an industrial hall with a height of 5000 mm, made at a scale of 1:10 by one of the authors of [32].

Therefore, the model was a square tube of 30 × 30 × 1.5 mm, with a height of 500 mm.

Figure 8 shows a summary of the measurements for T_{02} = (100;200;300;350;400;450; 500;600) °C nominal temperatures, where the position of the measurement points is given in percentages L_Ψ [%]. Taking into account the results of the authors' investigations in [30], Figures 9–11 show the three recommended intervals (L_I, L_{II}, L_{III}).

Moving to the coordinates for conventional temperatures T_Ψ [%], we obtain the curves in Figures 12–15 for the $T_\Psi - L_\Psi$ coordinates; this is first for the global curves, followed by those corresponding to the three previously mentioned intervals. Here, we can highlight the tendency of the dimensionless curves to approach each other, and starting from T_{02} = 500 °C, they can be treated as a single curve.

Based on these data, as a reference curve that at T_{02} = 500 °C in the model, we will be able to forecast, with regard to the points of the prototype that are homologous with the model, the temperature values corresponding to a T_{01} = 930 °C, according to relation (16).

Thus, following the replacement of the known values, namely T_{02} = 500 °C and T_{01} = 930 °C, each t_2^* value will correspond, based on relation (16), to the value of t_1^*

$$t_1^* = \frac{T_{01}}{T_{02}} \cdot t_2^* = \frac{930}{500} \cdot t_2^* = 1.86 \cdot t_2^* \tag{17}$$

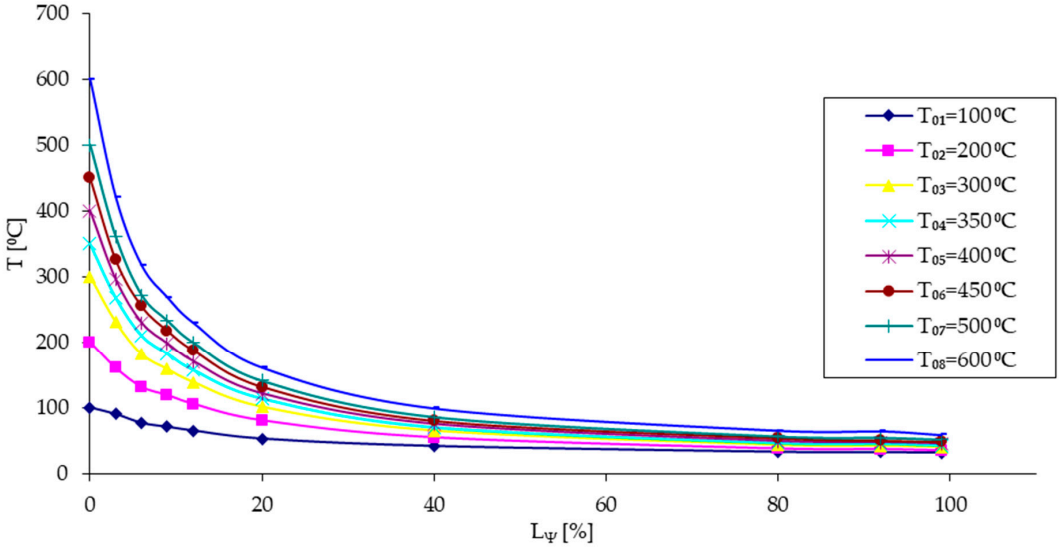

Figure 8. Complete column model heated at different $T_{02} = (100; 200; 300; 350; 400; 450; 500; 600)$ °C nominal temperatures in $T[°C] - L_\Psi[\%]$ coordinates.

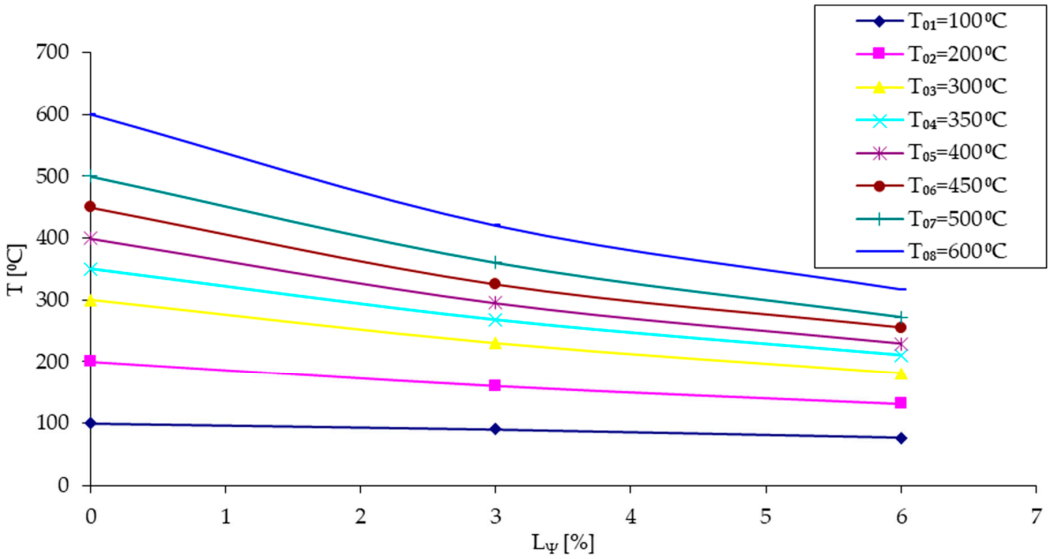

Figure 9. The first interval L_I for curves from Figure 8.

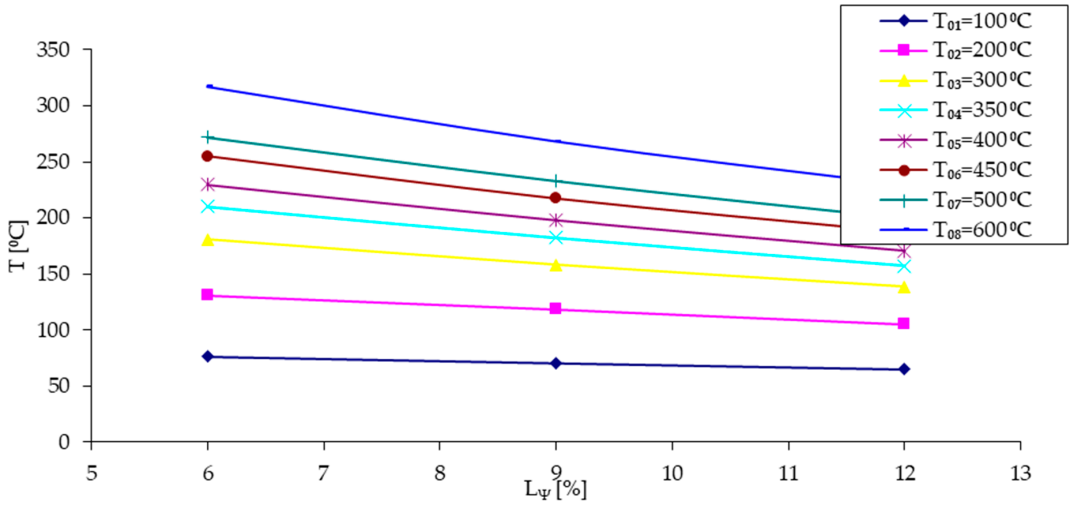

Figure 10. The second interval L_{II} for curves from Figure 8.

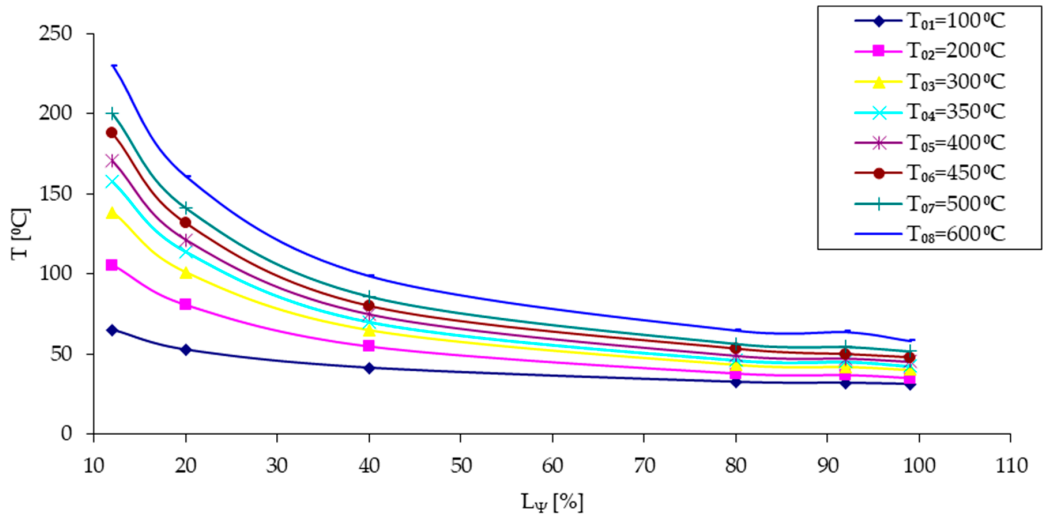

Figure 11. The third interval L_{III} for curves from Figure 8.

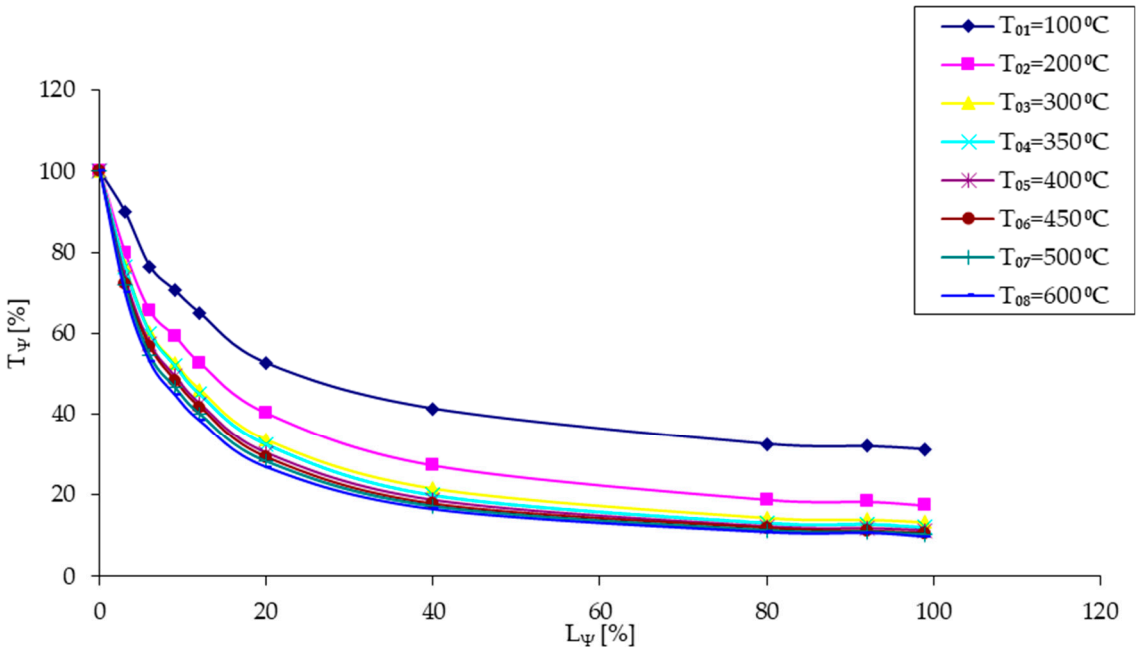

Figure 12. Complete column model heated at different $T_{02} = (100; 200; 300; 350; 400; 450; 500; 600)°C$ nominal temperatures in T_Ψ [%] − L_Ψ [%] coordinates.

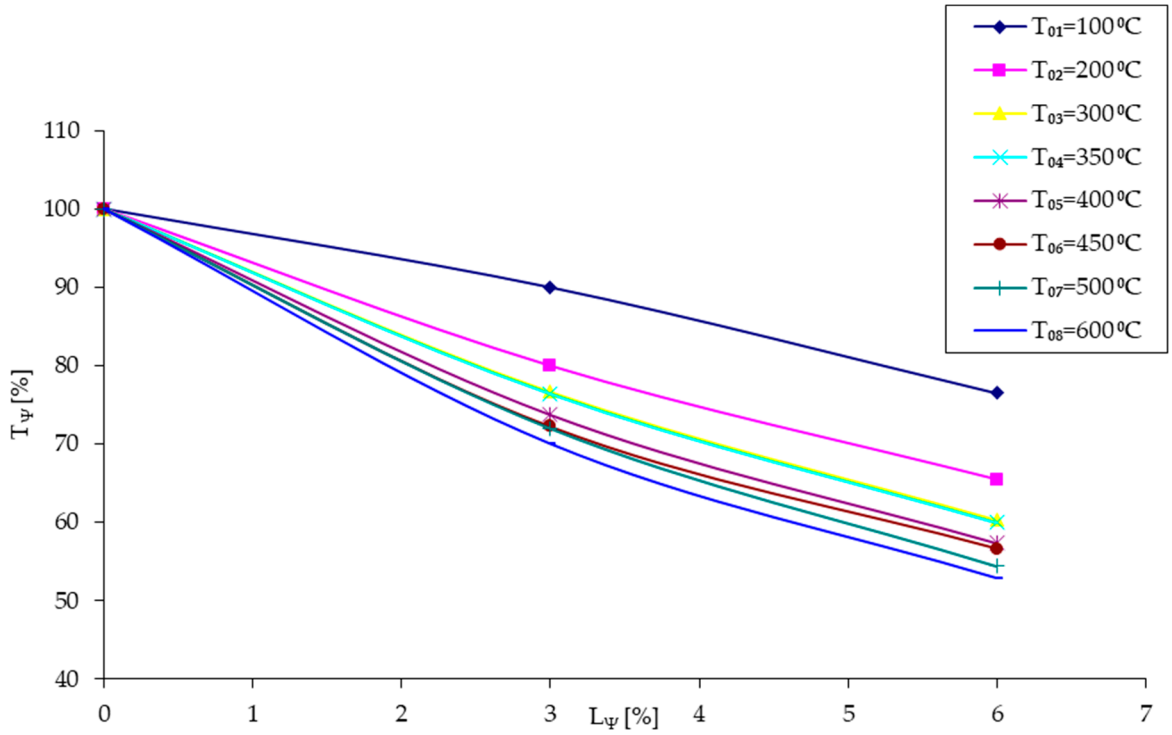

Figure 13. The first interval L_I for curves from Figure 12.

Figure 16 shows the reference curve related to the model (column 1) for T_{02} = 500 °C, and Figure 17 shows that of the predicate curve for the prototype (column 1) for T_{01} = 930 °C.

In the same way, let us now consider a model of an industrial hall made at a scale of 1:10, where the columns (columns) have dimensions of 30 × 30 × 1.5 mm and a height of 500 mm, and the beams (horizontal connecting elements) have a cross section of 10 × 1.5 mm (Figure 18).

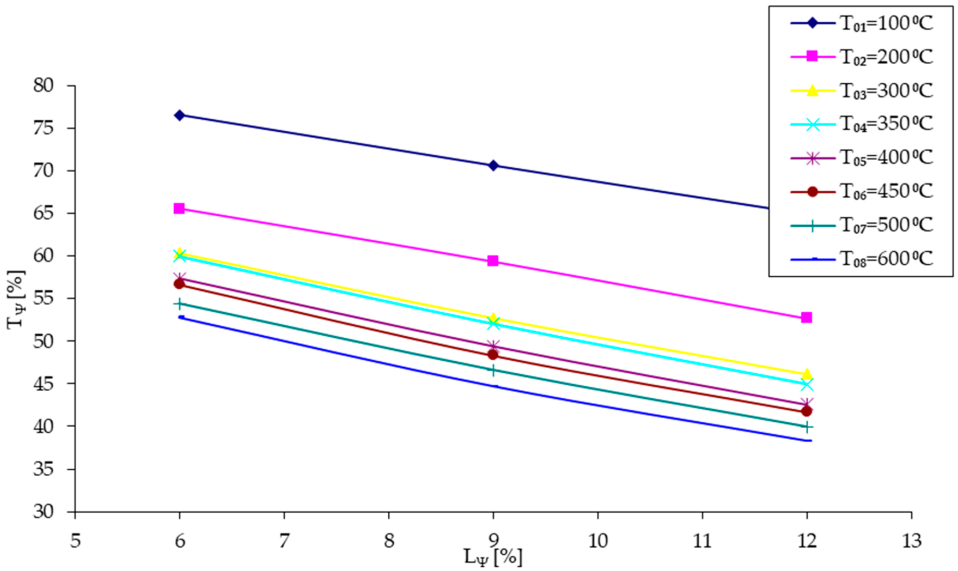

Figure 14. The second interval L_{II} for curves from Figure 12.

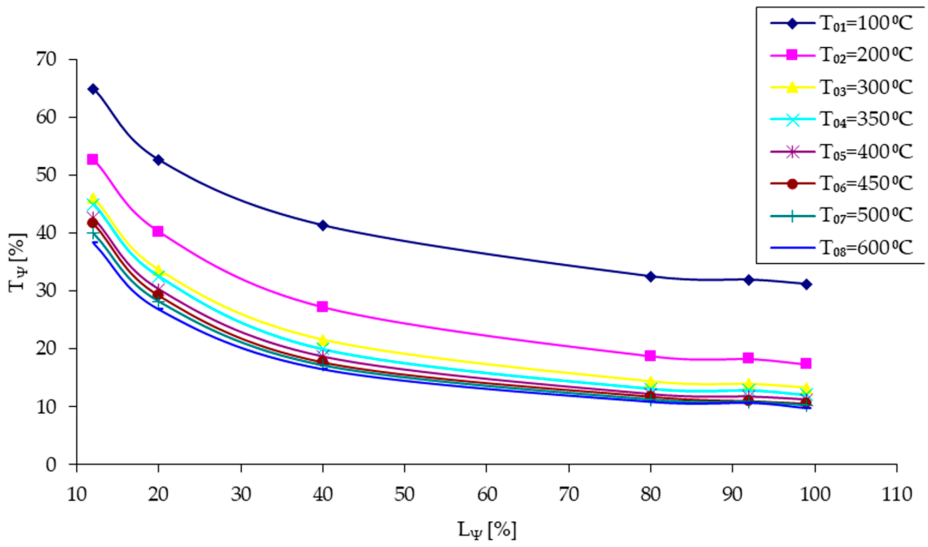

Figure 15. The third interval L_{III} for curves from Figure 12.

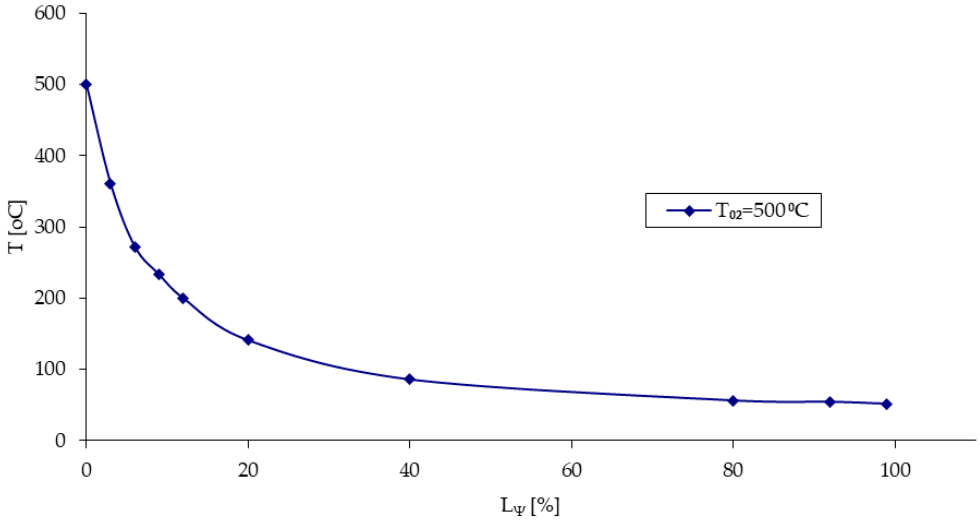

Figure 16. Column model tested at T_{02} = 500 °C.

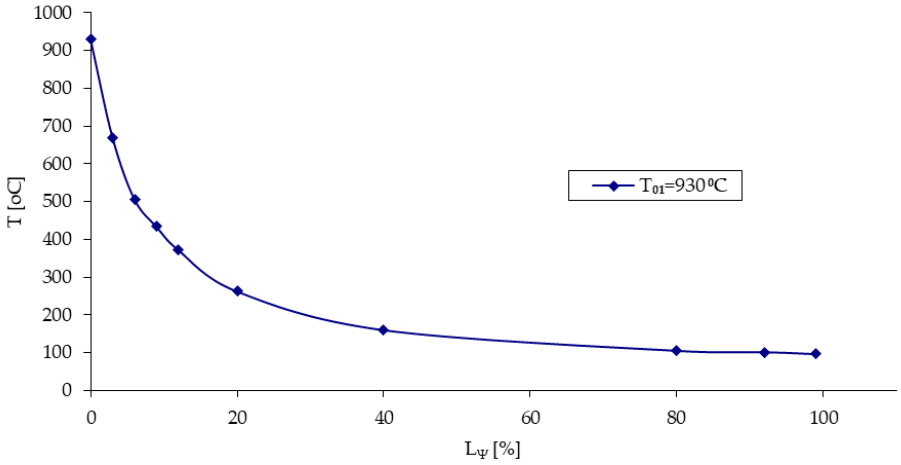

Figure 17. Prototype column forecasted at T_{01} = 930 °C.

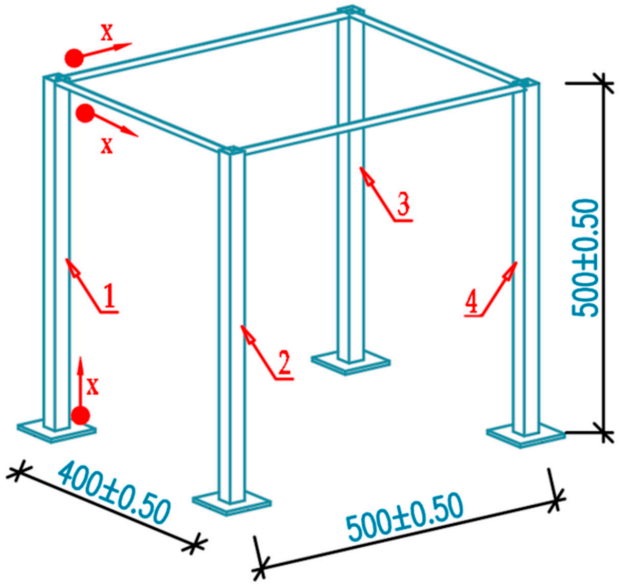

Figure 18. The model of an industrial hall made at a scale of 1:10.

Based on the reference temperature T_{02} = 500 °C, to which the model was heated at the level of column 1, for the beam connecting columns 1 and 4 (therefore, beam 1–4), the thermal values shown in Figure 19 were measured; these are set in $T[°C] - L_{\Psi}[\%]$ coordinates.

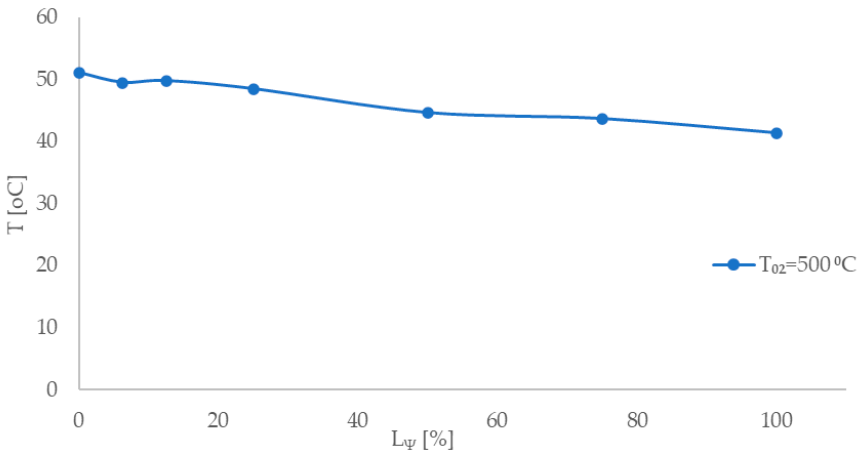

Figure 19. Temperature field in beam 1–4 of the model.

The homologous points on beam 1–4 of the prototype, considered to be heated at the reference temperature T_{01} = 930 °C at the level of real column 1, corresponded to the predicted thermal field in $T[°C] - L_{\Psi}[\%]$ coordinates; these are shown in Figure 20.

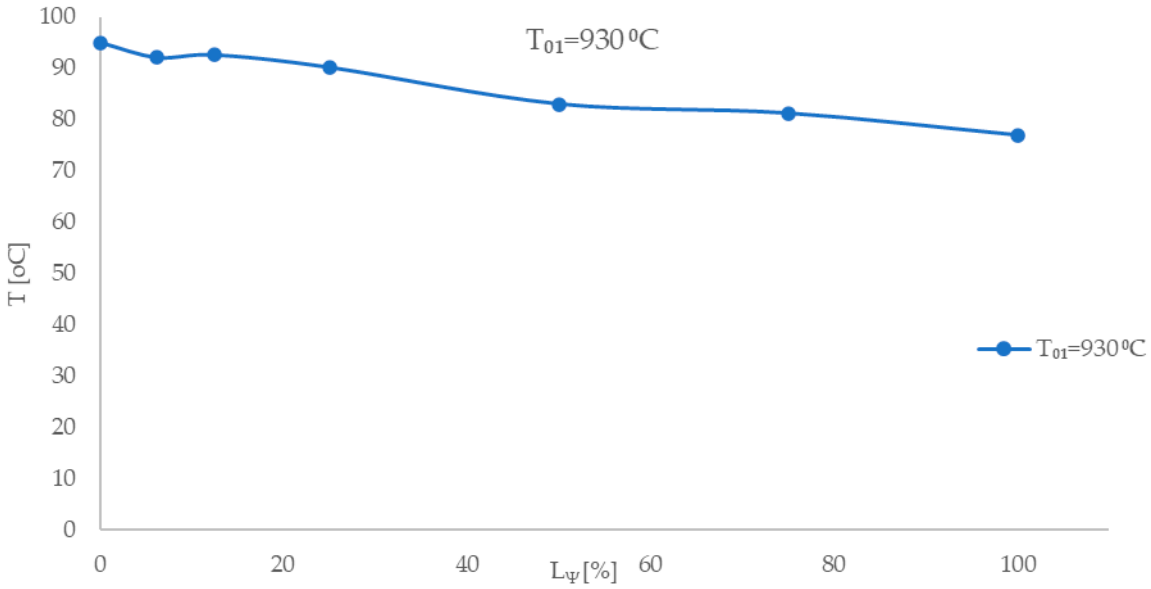

Figure 20. Temperature field in beam 1–4 of the prototype.

It can be seen that the MDA methodology/approach presented and illustrated above represents a potentially useful tool for construction specialists dealing with problems related to the thermal loading of buildings. The T_{Ψ} [%] $- L_{\Psi}$ [%] conventional curves help in simplifying and reducing the material and human costs related to the implementation of more flexible models in the study of complex phenomena, such as that of heat transfer in the structural elements of buildings with different purposes.

6. Limitations of the Research

The authors are aware that the results presented in this study represent only a first step in the long process of implementing the facilities offered by MDA. In this regard, this research has a number of limitations, which are listed below.

- The authors plan to extend their investigations with MDA to the real fire scenarios, where both the materials that cause the fire and those that burn once the fire breaks out will be considered;
- In this detailed study, the authors aim to involve specialists from various related fields, so that the chosen variables reflect all aspects of these real fire cases;
- Extending the authors' research to heat sources other than point sources will involve the design, construction, and testing of new stands (test benches), the efficiency of which will need to be verified and further improved/refined;
- The interaction between resistance structures and real fire sources will need to be thoroughly analyzed; this will enable the development of model laws, the results of which will be compared with those in the literature;
- The authors intend, in the near future, to carry out a comparative analysis of the results they obtained through MDA and those obtained through CDA, that is, through the equation approach and the law approach, which have been applied by specialists from all over the world.

7. Conclusions and Further Goals

- Regarding the results of these theoretical and experimental investigations, the authors address the following important aspects:
- The authors, based on an analysis of the main factors evaluated by specialists, highlight a series of aspects that may be related to the dimensional approaches currently used, namely GA, TS, and CDA, including their advantages and limits;
- By briefly analyzing MDA and illustrating its methodology, the authors believe that MDA can represent a useful means of investigation for any specialist in the field, at least with these results. This is particularly with reference to the point source of heat;
- In this study, from the set of variables, the authors analyzed the beneficial effects of choosing some as independent and dependent variables, respectively;
- By introducing a new conventional coordinate system, $T_\Psi - L_\Psi$, a new, more efficient approach to the prototype–model correlation becomes possible. This is based on the detailed experimental investigation carried out exclusively on the attached model at more advantageous (lower) temperatures, such as 500 °C;
- The authors proved that if the model is subjected to thermal regimes up to a temperature of 500 °C, then these conventional $T_\Psi - L_\Psi$ curves will be able to estimate the behavior of the prototype well;
- The FEM results were in relatively good agreement with the experimental results;
- However, numerical modelling is not able to describe the phenomenon of the stabilized temperature and consequently demands supplementary experimental investigations to establish the whole set of parameters for the numerical modelling of three zones, at minimum.
- The MLs deduced for double symmetrical cross-sectional structural elements can be applied without any difficulties to the whole structure, which is obtained from elements of the type analyzed before, by a simple extension of the dependent variables in matrix B; this takes into consideration the behavior of the homologous points analyzed by the authors.

Based on these results, the authors intend to continue their theoretical and experimental research by focusing on the following aspects:

- Considering that the model laws can be obtained not only via a parametric approach (such as MDA) but also via equations and law approaches, the authors intend to perform a comparative analysis (theoretical and experimental) of their own MLs with dimensionless quantities in the abovementioned approaches in real fire scenarios. In the authors' opinion, the results of these comparisons will be of interest to specialists and enable them to improve their own MDA approach in the context of real fires.
- The results obtained can be extended to other significant structural elements subjected to fire;
- The MDA approach can be involved in the methodology used to describe complex fires, verifying if the elements of ML, such as the entire deduced ML, remain valid for these complex burning phenomena;
- A generalization of the MDA methodology regarding structural elements with an asymmetric cross-section could also be carried out in the near future by the authors;
- Similarly, FEM results can also be involved in this extension/generalization process;
- In addition, based on the measurement results, it can be proven whether the FEM model is adequate or needs to be improved for a more accurate description of heat flux propagation;
- The authors also propose the establishment of databases using these theoretical and experimental results to help designers and specialists in the field;

- In addition, MDA can also be used in the fire protection of different sorts of materials, including steel, but also those with a suitable λ thermal conductivity; in this sense, the inferred MLs need to be revalidated via other, more suitable experimental investigations.

Author Contributions: Conceptualization, I.S. and T.-F.G.; methodology, I.S.; software, B.B.; validation, I.-R.S. and K.J.; formal analysis, B.B.; investigation, I.S. and I.-R.S.; resources, I.S.; data curation, I.-R.S.; writing—original draft preparation, I.S., B.B., K.J. and D.-E.M.; writing—reviewing and editing, B.B., K.J. and D.-E.M.; visualization, B.B.; supervision, K.J. All authors have read and agreed to the published version of the manuscript.

Funding: This research received no external funding.

Data Availability Statement: All important data from this research are available in this paper.

Conflicts of Interest: The authors declare no conflicts of interest.

References

1. Szirtes, T. *Applied Dimensional Analysis and Modelling*; McGraw-Hill: Toronto, ON, Canada, 1998.
2. Maślak, M.; Pazdanowski, M.; Woźniczka, P. Numerical Validation of Selected Computer Programs in Nonlinear Analysis of Steel Frame Exposed to Fire. In *Computer Methods in Mechanics (CMM2017), Proceedings of the 22nd International Conference on Computer Methods in Mechanics, Lublin, Poland, 13–16 September 2017*; AIP Publishing: Melville, NY, USA, 2018; Volume 1922, pp. 150007-1–150007-9. [CrossRef]
3. de Silva, D.; Nuzzo, I.; Nigro, E.; Occhiuzzi, A. Intumescent Coatings for Fire Resistance of Steel Structures: Current Approaches for Qualification and Design. *Coatings* **2022**, *12*, 696. [CrossRef]
4. Sharma, P.; Quintiere, G.J. Compartment Fire Temperatures. *J. Fire Prot. Eng.* **2010**, *20*, 4. [CrossRef]
5. Deal, S.; Craig, L.; Beyler, L.C. Correlating Preflashover Room Fire Temperatures. *J. Fire Prot. Eng.* **1990**, *2*, 33–48. [CrossRef]
6. Hsu, S.Y.; T'ien, S.J.; Takahashi, F.; Olson, S. Modelling Heat Transfer in Thin Fire Blanket Materials under High External Heat Fluxes. *Fire Saf. Sci.* **2011**, *10*, 973–986. [CrossRef]
7. Bükülmez, P.S.; Celik, O.C. Pre and post-fire mechanical properties of structural steel and concrete in steel-concrete composite cellular beams. *MATEC Web Conf.* **2019**, *282*, 02054. [CrossRef]
8. Quintiere, J.G. Scaling realistic fire scenarios. *Prog. Scale Model. Int. J.* **2020**, *1*, 1. [CrossRef]
9. Andreozzi, A.; Bianco, N.; Musto, M.; Rotondo, G. Scaled models in the analysis of fire-structure Interaction. *J. Phys. Conf. Ser.* **2015**, *655*, 012053. [CrossRef]
10. Quintiere, J.G. Scaling Applications in Fire Research. *Fire Saf. J.* **1989**, *15*, 3–29. [CrossRef]
11. Quintier, G.J. *Fundamentals of Fire Phenomena*; John Willey & Sons: Hoboken, NJ, USA, 2006.
12. Saito, K.; Williams, F.A. Scale Modeling in the Age of High-Speed Computation. In *Progress in Scale Modeling: Selections from the International Symposia on Scale Modeling, ISSM VI (2009) and ISSM VII (2013)*; Saito, K., Ito, A., Nakamura, Y., Kuwana, K., Eds.; Springer: Cham, Switzerland, 2014; Volume 2, pp. 1–18. [CrossRef]
13. Barr, D.I.H. Consolidation of Basics of Dimensional Analysis. *J. Eng. Mech.* **1984**, *110*, 1357–1376. [CrossRef]
14. Bhaskar, R.; Nigam, A. Qualitative Physics using Dimensional Analysis. *Artif. Intell.* **1990**, *45*, 73–111. [CrossRef]
15. Carinena, J.F.; Santander, M. Dimensional Analysis. *Adv. Electron. Electron Phys.* **1988**, *72*, 181–258.
16. Carlson, D.E. Some New Results in Dimensional Analysis. *Arch. Ration. Mech. Anal.* **1978**, *68*, 191–210. [CrossRef]
17. Gibbings, J.C. A Logic of Dimensional Analysis. *J. Phys. A Math. Gen.* **1982**, *15*, 1991–2002. [CrossRef]
18. Buckingham, E. On Physically Similar Systems. *Phys. Rev.* **1914**, *4*, 345. [CrossRef]
19. Szekeres, P. Mathematical Foundations of Dimensional Analysis and the Question of Fundamental Units. *Int. J. Theor. Phys.* **1978**, *17*, 957–974. [CrossRef]
20. Schnittger, J.R. Dimensional Analysis in Design. *J. Vib. Accoust. Stress Reliab.* **1988**, *110*, 401–407. [CrossRef]
21. Coyle, R.G.; Ballicolay, B. Concepts and Software for Dimensional Analysis in Modelling. *IEEE Trans. Syst. Man Cybern.* **1984**, *14*, 478–487. [CrossRef]
22. Canagaratna, S.G. Is dimensional analysis the best we offer. *J. Chem. Educ.* **1993**, *70*, 40–43. [CrossRef]
23. Alshqirate, A.A.Z.S.; Tarawneh, M.; Hammad, M. Dimensional Analysis and Empirical Correlations for Heat Transfer and Pressure Drop in Condensation and Evaporation Processes of Flow Inside Micropipes: Case Study with Carbon Dioxide (CO_2). *J. Braz. Soc. Mech. Sci. Eng.* **2012**, *34*, 89–96.
24. Islam, M.F.; Lye, L.M. Combined use of dimensional analysis and modern experimental design methodologies in hydrodynamics experiments. *Ocean Eng.* **2009**, *36*, 237–247. [CrossRef]

25. Jofre, L.; del Rosario, Z.R.; Iaccarino, G. Data-driven dimensional analysis of heat transfer in irradiated particle-laden turbulent flow. *Int. J. Multiph. Flow* **2020**, *125*, 103198. [CrossRef]
26. Yao, S.; Yan, K.; Lu, S.; Xu, P. Prediction and application of energy absorption characteristics of thin-walled circular tubes based on dimensional analysis. *Thin-Walled Struct.* **2018**, *130*, 505–519. [CrossRef]
27. Pankhurst, R.C. *Dimensional Analysis and Scale Factor*; Chapman & Hall Ltd.: London, UK, 1964.
28. Száva, R.I.; Bolló, B.; Bencs, P.; Jármai, K.; Száva, I.; Popa, G.; Asztalos, Z.; Vlase, S. Experimental and Numerical Studies of the Heat Transfer in Thin-walled Rectangular Tubes under Fire. *Symmetry* **2022**, *14*, 1781. [CrossRef]
29. Turzó, G. Temperature distribution along a straight bar sticking out from a heated plane surface and the heat flow transmitted by this bar (I)-Theoretical Approach. *Ann. Fac. Eng. Hunedoara-Int. J. Eng.* **2016**, *14*, 49–53.
30. Turzó, G.; Száva, R.I.; Dancsó, P.; Száva, I.; Vlase, S.; Munteanu, V.M.; Gălățanu, T.F.; Asztalos, Z. A New Approach in Heat Transfer Analysis: Reduced-Scale Straight Bars with Massive and Square-Tubular, Cross-Sections. *Mathematics* **2022**, *10*, 3680. [CrossRef]
31. Dani, P. Theoretical and Experimental Study of Heat-Field Propagation Through Multi-Layer Fire-Protection on Stress-, and Strain-State of Metallic Structures. Ph.D. Thesis, Transilvania University of Brasov, Brasov, Romania, 2011.
32. Munteanu, I.R. Investigation Concerning Temperature Field Propagation Along Reduced Scale Modelled Metal Structures. Ph.D. Thesis, Transilvania University of Brasov, Brasov, Romania, 2018.